Global Change Biology

Global Change Biology (2014) 20, 1585–1603, doi: 10.1111/gcb.12465

Controls on water balance of shallow thermokarst lakes and their relations with catchment characteristics: a multi-year, landscape-scale assessment based on water isotope tracers and remote sensing in Old Crow Flats, Yukon (Canada)

KEVIN W. TURNER[1,2], BRENT B. WOLFE[1], THOMAS W. D. EDWARDS[3], TREVOR C. LANTZ[4], ROLAND I. HALL[5] and GUILLAUME LAROCQUE[6]

[1]*Department of Geography and Environmental Studies, Wilfrid Laurier University, Waterloo, ON N2L 3C5, Canada,* [2]*Department of Geography, Brock University, St. Catharines, ON L2S 3A1, Canada,* [3]*Department of Earth and Environmental Sciences, University of Waterloo, Waterloo, ON N2L 3G1, Canada,* [4]*School of Environmental Studies, University of Victoria, Victoria, BC V8P 5C2, Canada,* [5]*Department of Biology, University of Waterloo, Waterloo, ON N2L 3G1, Canada,* [6]*Quebec Centre for Biodiversity Science, Biology Department, McGill University, Montreal, QC H3A 1B1, Canada*

Abstract

Many northern lake-rich regions are undergoing pronounced hydrological change, yet inadequate knowledge of the drivers of these landscape-scale responses hampers our ability to predict future conditions. We address this challenge in the thermokarst landscape of Old Crow Flats (OCF) using a combination of remote sensing imagery and monitoring of stable isotope compositions of lake waters over three thaw seasons (2007–2009). Quantitative analysis confirmed that the hydrological behavior of lakes is strongly influenced by catchment vegetation and physiography. Catchments of snowmelt-dominated lakes, typically located in southern peripheral areas of OCF, encompass high proportions of woodland/forest and tall shrub vegetation (mean percent land cover = ca. 60%). These land cover types effectively capture snow and generate abundant snowmelt runoff that offsets lake water evaporation. Rainfall-dominated lakes that are not strongly influenced by evaporation are typically located in eastern and northern OCF where their catchments have higher proportions of dwarf shrub/herbaceous and sparse vegetation (ca. 45%), as well as surface water (ca. 20%). Evaporation-dominated lakes, are located in the OCF interior where their catchments are distinguished by substantially higher lake area to catchment area ratios (LA/CA = ca. 29%) compared to low evaporation-influenced rainfall-dominated (ca. 10%) and snowmelt-dominated (ca. 4%) lakes. Lakes whose catchments contain >75% combined dwarf shrub/herbaceous vegetation and surface water are most susceptible to evaporative lake-level drawdown, especially following periods of low precipitation. Findings indicate that multiple hydrological trajectories are probable in response to climate-driven changes in precipitation amount and seasonality, vegetation composition, and thermokarst processes. These will likely include a shift to greater snowmelt influence in catchments experiencing expansion of tall shrubs, greater influence from evaporation in catchments having higher proportions of surface water, and an increase in the rate of thermokarst lake expansion and probability of drainage. Local observations suggest that some of these changes are already underway.

Keywords: climate change, hydrology, isotope tracers, land cover, Old Crow Flats, remote sensing, spatial analysis, thermokarst lakes

Received 24 May 2013; revised version received 27 August 2013 and accepted 17 September 2013

Introduction

Northern high latitudes contain numerous lake-rich landscapes, which host abundant wildlife and support northern communities. Evidence suggests that thermokarst landscapes are particularly vulnerable to variations in climate. For example, observations in Siberia and Alaska based on remote sensing indicate widespread reductions in lake surface area within discontinuous permafrost zones (Yoshikawa & Hinzman, 2003; Smith *et al.*, 2005; Riordan *et al.*, 2006), and surface-water accumulation and lake expansion in areas of continuous permafrost during recent decades (Smith *et al.*, 2005; Jorgenson *et al.*, 2006). Residents have made similar observations in Alaska (Hinkel *et al.*, 2007) and northern Canada (ABEK Co-op, 2007), and there are concerns that landscape responses to changing hydrological conditions

Correspondence: Kevin W. Turner, tel. +1 905 688 5550, fax +1 905 688 6369, e-mail: kturner2@brocku.ca

will reduce their ability to sustain traditional ways of life. These observations have been linked to recent changes in climate. For example, the acceleration of thermokarst processes, including lake expansion (Smith *et al*., 2005), ponding (Jorgenson *et al*., 2006; Rowland *et al*., 2010) and vertical drainage of ponds through taliks (Yoshikawa & Hinzman, 2003), has been associated with increased temperature and/or precipitation. Lake water-level reductions have also been attributed to increased evaporation (Labrecque *et al*., 2009). Despite these observed trends, the relative importance of hydrological processes on the water balances of thermokarst lakes and ponds at the landscape scale remains largely unknown because effects of climatic variations may be highly lake-specific and difficult to decipher using remote-sensing measurements alone (Plug *et al*., 2008; Carroll *et al*., 2011; MacDonald *et al*., 2012). Observations showing that hydrological changes are not uniform at the landscape scale (Turner *et al*., 2010; Rover *et al*., 2012; Jepsen *et al*., 2013) underscore the need to identify drivers of spatial and temporal variability in the responses of lake water balance to climate. This knowledge will strengthen our ability to predict how thermokarst landscapes may evolve in the future under different climate-change scenarios.

Recent studies have provided important insights into the hydrological processes associated with thermokarst lakes (e.g., Marsh & Neumann, 2001; Pohl *et al*., 2009; Marsh *et al*., 2010), although these are often limited to a small number of basins and are unable to address hydrological variability that may exist among lakes at the landscape scale. Advances in observations and process-based studies are needed since conventional hydrological approaches require instrumentation that is challenging to implement over broad, remote regions (Rowland *et al*., 2010). The need to develop an improved understanding of linkages among climate, landscape characteristics and hydrology is compounded by the notion that these landscapes are in a transitional state and uncertainty about whether current processes that drive hydrological change will differ in the future (Rowland *et al*., 2010; Avis *et al*., 2011).

Old Crow Flats (OCF; Fig. 1) is a lake-rich thermokarst landscape spanning 5600 km^2 in northern Yukon, Canada, where local land-users have observed profound environmental changes including changing water levels and increased shrub cover over recent decades (ABEK Co-op, 2007). Recognized as a Ramsar Wetland of International Importance (The Ramsar

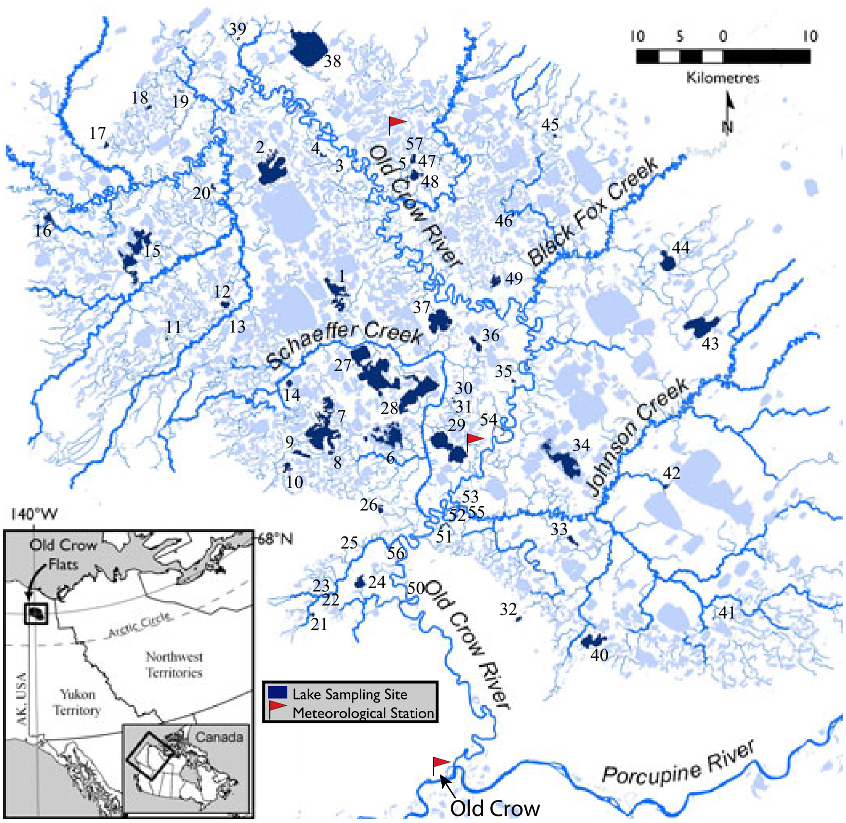

Fig. 1 Map showing locations of the town of Old Crow (Yukon, Canada), the Old Crow Flats, the 57 study lakes (numbered) and meteorological stations (flags).

Convention on Wetlands, 1982), OCF straddles the boreal-tundra transition zone and contains ca. 2700 very shallow (mean = ca. 1.5 m) lakes that are predominantly thermokarst in origin. In addition to surface water, broad land cover types in OCF comprise tall shrubs, spruce forest, and tundra vegetation. Exposed bare rock is present in surrounding upland areas. OCF supports abundant wildlife, which is an integral component of the indigenous Vuntut Gwitchin First Nation (VGFN) culture. The VGFN have thrived in this area for many generations and have recently become concerned about the impact that hydrological and landscape changes will have on wildlife populations, and their traditional lifestyle (Wolfe *et al.*, 2011a).

To address these concerns, an initial assessment of the relative importance of hydrological processes on water balances of lakes in OCF was undertaken for the 2007 ice-free season (June–September) using water isotope tracers (Turner *et al.*, 2010). Results highlighted strong diversity in lake hydrology, attributed to differences in catchment vegetation. For example, lakes located in areas of forest vegetation tended to receive greater snowmelt, whereas lakes in areas of tundra vegetation were fed primarily by rainfall and experienced greater evaporation. Here, we further characterize and test these relations by integrating spatial analysis of individual catchment vegetation type and surface water area, and hydrological characteristics of the same 56 lakes and one other lake. Additionally, we probed the persistence of these relations over multiple years (2007–2009) and, thus, also address the role of seasonal and interannual variations in meteorological conditions on lake hydrology. These findings present an opportunity to anticipate future lake hydrological trajectories in OCF under different climate regimes. The approaches we utilize here are readily transferable to other northern landscapes.

Materials and methods

Meteorological data

Meteorological data from four stations at three locations were used in this study (Fig. 1). Two stations were located at the Old Crow airport, located ca. 25 km south of OCF. One of the stations was maintained by Environment Canada (since 1951) and a second ['Wilfrid Laurier University (WLU) station'] was installed on 7 June 2007 for the duration of the study. Data used from the Environment Canada station included hourly temperature, snow water equivalent, and rainfall, while the WLU station provided hourly temperature, relative humidity and rainfall. A third meteorological station was deployed in the central OCF ('John Charlie Lake') on 14 June 2008, ca. 35 km north of Old Crow, and provided the same parameters as the WLU station. Rainfall data (22 June 2006–17 July 2009) were obtained from a fourth meteorological station in the northern OCF in Vuntut National Park (Parks Canada). Comparisons of common parameters among all stations for overlapping time periods were used to evaluate the suitability of data recorded in Old Crow to represent meteorological conditions in OCF. Precipitation estimates for OCF were derived from the Environment Canada meteorological station.

Land cover classification and lake catchment delineation

A land-cover map was obtained by performing a supervised classification of a Landsat 5 TM mosaic. To generate a cloud-free mosaic covering the entire study area, six Landsat images from July and August 2007 (US Geological Survey) were cropped and assembled using the IDRISI software package (Eastman, 2009). A series of oblique aerial and ground photographs, airborne videos, and vegetation field surveys of the study area were used to define training sites for the land-cover classification. Classes included coniferous and deciduous woodland/forest, tall shrub vegetation, herbaceous plants, non-vascular plants, dwarf shrub, exposed rock/sand, fire scar/barrens, lakes, ponds, streams, wetlands, and floating vegetation. Urban development is absent from OCF. The supervised classification was performed using the maximum likelihood procedure (MAXLIKE) in the Idrisi software package.

To simplify this land cover to a level of detail appropriate for this study, classes were combined into the following aggregated categories (Fig. 2): (i) woodland/forest vegetation; (ii) tall shrub vegetation; (iii) dwarf shrub/herbaceous (including non-vascular) vegetation; (iv) sparse vegetation (exposed rock/sand, barrens); and (v) surface water (lakes, ponds, streams, wetlands, floating vegetation). Accuracy of land cover classifications was tested through ground-truthing (80 field sites) and sites identified on oblique aerial photographs ($n = 920$). Overall classification accuracy was 69% (Kappa statistic = 0.58). Results show that surface water was the most accurate (89%), followed by sparse vegetation (78%), dwarf shrub/herbaceous vegetation (63%), forest/woodland vegetation (51%), and tall shrub vegetation (39%) (T. Lantz, unpublished data).

The catchments of each of the 57 study lakes were delineated using a digital elevation model (30 m resolution; available from Yukon Geomatics, http://www.geomaticsyukon.ca/data/datasets), a SPOT 5 (Système Pour l'Observation de la Terre) image acquired in July 2007, Canadian National Topographic Database vector data showing creek locations (available from Natural Resources Canada, http://geogratis.cgdi.gc.ca/), oblique aerial photographs and field observations. Portions of catchments within peripheral headwater locations were easily distinguishable as elevation changes and the location of stream networks were highly visible in the available spatial data. However, digitizing catchments in low-relief areas required reference to field observations and geo-referenced oblique aerial photographs to assess locations of creeks and fens around the study lakes. Where no hydrological connection was apparent between adjacent lakes, a

Fig. 2 Oblique aerial photographs of example lake catchments that vary in proportion of land cover types (i.e., woodland/forest vegetation, tall shrub vegetation, dwarf shrub/herbaceous vegetation, sparse vegetation, and surface water).

catchment boundary was assumed to bisect the terrestrial area between water bodies.

Water isotope sampling and analyses

With the aid of a helicopter, surface water was sampled from the 57 study lakes (Fig. 1) nine times over the 2007–2009 ice-free seasons, except in September 2007 when only 27 lakes were sampled due to poor weather conditions. Samples were obtained in early June (6–13), late July (22–26) and September/October (September 29 – October 4 in 2007; September 4–6 in 2008 and 2009). Lake selection aimed to capture the hydrological diversity present in the landscape and included lakes of varying physical characteristics (e.g., size and water clarity; for additional site description, see Turner *et al.*, 2010). Several lakes included in this study were selected during a research-planning workshop with local residents, many of whom have observed recent hydrological change (Wolfe *et al.*, 2011b).

Water samples were collected at 10-cm water depth in 30-ml high-density polyethylene bottles and transported to the University of Waterloo Environmental Isotope Laboratory (UW-EIL) for determination of oxygen and hydrogen isotope composition using conventional techniques (Epstein & Mayeda, 1953; Morrison *et al.*, 2001). Isotopic compositions are expressed as δ-values, representing deviations in per mil (‰) from Vienna Standard Mean Ocean Water (VSMOW) such that $\delta_{\mathrm{sample}} = [(R_{\mathrm{sample}}/R_{\mathrm{VSMOW}}) - 1] \times 10^3$, where R is the $^{18}O/^{16}O$ or $^{2}H/^{1}H$ ratio in sample and VSMOW. Results of $\delta^{18}O$ and $\delta^{2}H$ analyses are normalized to −55.5‰ and −428‰, respectively, for Standard Light Antarctic Precipitation (Coplen, 1996). Analytical uncertainties are ±0.2‰ for $\delta^{18}O$ and ±2.0‰ for $\delta^{2}H$.

A class-A evaporation pan was deployed and maintained at the Old Crow airport during the 2007–2009 ice-free seasons to simulate isotopic behavior of a terminal lake (i.e., a closed-drainage basin at isotopic and hydrological steady state where evaporation equals inflow). Pan water volume was maintained weekly. Water used to refill the pan was obtained from the community well, which taps sub-permafrost groundwater having a constant isotopic composition. After refilling each week, the pan water was mixed manually and a 30-ml water sample was taken for isotopic analysis.

Lake hydrological conditions, including the relative importance of source water type (i.e., snowmelt vs. rainfall) and evaporation relative to inflow (E/I), were determined for each lake at the time of sampling. The isotopic composition of source water (δ_I), which was related to the proportion of snowmelt vs. rainfall, and E/I values were derived using the coupled-isotope tracer approach developed by Yi *et al.* (2008). These approaches are based on the linear resistance model of Craig & Gordon (1965) (see Supporting Information) and have been used elsewhere for determining lake hydrological patterns in freshwater landscapes (e.g., Brock *et al.*, 2009). For each lake, δ_I is assumed to plot at the intersection of the Global Meteoric Water Line (GMWL) and the lake-specific evaporation line (see Fig 4b in Yi *et al.*, 2008). Lake input classifications were defined by δ_I relative to the mean annual isotope composition of precipitation (δ_P), where $\delta_I \leq \delta_P$ for snowmelt-dominated lakes and $\delta_I > \delta_P$ for rainfall-dominated lakes (Turner *et al.*, 2010). E/I values represent the relative importance of evaporation on lakes. We designated lakes with E/I > 0.5 as evaporation-dominated, which were mostly a subset of rainfall-dominated lakes. This threshold, which was modified from the value of 1.0 used in Turner *et al.* (2010), was used to explore gradients of evaporation with catchment characteristics. E/I values are modeled based on the assumption that lakes are well-mixed and at quasi-steady-state, thus values >1 are not physically meaningful, but have comparative value.

Inverse-distance-weighted interpolation methods were used to map spatial distributions of δ_I and E/I values. We verified the level of spatial association among δ_I and E/I values using calculated Moran's *I* coefficients (Anselin, 1995) for each sampling period. The level of positive spatial association is expressed on a scale from 0 (weakest) to 1 (strongest). Spatial analysis was not performed for the September 2007 data set due to the low number of lakes sampled.

Multivariate ordination by principal components analysis (PCA) was used to assess relations among catchment land cover characteristics (percent cover by woodland/forest vegetation, tall shrub vegetation, dwarf shrub/herbaceous vegetation, sparse vegetation, and surface water) and hydrological conditions. To identify the hydrological conditions associated with catchment land cover characteristics, sample scores were coded within the ordination plot based on lake hydrological classifications (snowmelt-dominated, rainfall-dominated, and evaporation-dominated) and further distinguished by E/I ratio. Average mid-summer (July) conditions over the three-year sampling period were used to categorize the lakes. The PCA was performed using the Stats package for the software R (version 2.8.1; R Core Team, 2012). An analysis of similarities test (ANOSIM) was used to determine if catchment characteristics differ significantly among snowmelt, rainfall-, and evaporation-dominated lake hydrological categories. Land cover proportions for each catchment were square-root transformed prior to calculating the Bray-Curtis similarity coefficients used in the ANOSIM test. The ANOSIM test statistic (global R) ranges from 0 to 1, reflecting the observed differences between groups of samples compared to the differences among replicates within each group. A value of 0 indicates that the similarity between and within hydrological categories is the same on average, while a value of 1 indicates that replicates within a group are more similar to each other than to all other replicates of other groups (Clarke & Warwick, 2001). Pairwise testing was used to identify the level of variation in land cover characteristics among catchments of each hydrological category. P-values were computed by comparing the distribution of within- and across-group rank Bray-Curtis similarities (99 999 computations) to the initial rank similarity, as reported by the global R value (Clarke & Warwick, 2001; Clarke & Gorley, 2006). For all tests, we set alpha = 0.05. The ANOSIM test was performed using the software PRIMER version 6.1.5 (Clarke & Warwick, 2001; Clarke & Gorley, 2006).

Results

Meteorological conditions

Meteorological data were compared using a Student's *t*-test (available in the Stats package for R Software) to evaluate the uncertainty associated with using data recorded at the Old Crow airport to represent meteorological conditions in OCF (Fig. 3). During 2008–2009, temperatures recorded at the Old Crow airport meteorological stations (Environment Canada and WLU) were statistically similar to temperatures recorded in OCF (John Charlie Lake; *t*-test $P = 0.2631$). Relative humidity at the Old Crow airport (WLU station) closely tracked values in OCF (John Charlie Lake) in the early 2008 and late 2009 ice-free seasons. However, values between these stations were not statistically similar due to slightly lower values in OCF late in each season (*t*-test $P = 0.00004$). Higher relative humidity values in OCF may be due to a build-up of local atmospheric moisture produced by lake evaporation. Similar values for cumulative precipitation were obtained among meteorological stations located in Old Crow and OCF. Since the temperature and relative humidity records at the Old Crow airport extend throughout the duration of study (2007–2009) and correspond moderately well with data from OCF (Fig. 3a and b), the Old Crow airport meteorological data from the WLU station were used for development of the isotopic reference framework, as described below (see *Isotope hydrology*). Temperature and relative humidity recorded by the WLU station were flux-weighted according to the recommendations of Gibson (2002), based on potential evapotranspiration (Thornthwaite, 1948), and were used to constrain key reference points and analytical metrics within the isotopic framework (see below).

Patterns of seasonal variability in temperature and relative humidity were similar during the three-year monitoring period (Fig. 3a and b). Mean ice-free season temperature recorded by the WLU station at the Old Crow airport was slightly warmer in 2007 (14.4 °C) compared to 2008 (12.6 °C) and 2009 (12.7 °C). Mean temperatures recorded by Environment Canada (2009) during the 2007–2009 ice-free seasons for June (14.0 °C) and July (15.4 °C) were slightly above long-term mean monthly values since 1952 (12.5 °C and 14.5 °C, respectively) and confidence intervals calculated for the historical record (June: 12.08–13.08 °C and July: 14.08–14.87 °C). Mean August temperature for 2007–2009 (10.2 °C) was comparable to long-term mean monthly values since 1952 (10.7 °C) and within the calculated confidence interval (10.06–11.23 °C). Mean (flux-weighted) ice-free season relative humidity was slightly higher in 2008 (64.0%) and 2009 (66.5%) compared to 2007 (62.6%).

Annual precipitation between 2006 and 2009 was more variable than temperature and humidity (Fig. 3c). The 2006 ice-free season was characterized by above-average rainfall (190 mm; 1952-2009 mean (complete years) = 166 mm; Environment Canada, 2009) with near-record high rainfall in August (86 mm). The 2006–2007 winter experienced above-average snowfall (snow water equivalent (SWE) = 148 mm; 1951-2009 mean SWE = 100 mm; Environment Canada, 2009). Near-record three-month (March-May 2007) cumulative precipitation (96 mm), which preceded the first sampling campaign (June 2007), was almost three times greater than the 1951–2009 mean (34 mm). The latter half of May 2007 experienced ca. 22 mm of rain with 10 mm falling on 31 May, 1 one week prior to sampling. In contrast, below-average cumulative rainfall (111 mm) occurred during the subsequent ice-free months in 2007, followed by extremely low snowfall throughout the ice-covered months of 2007–2008 (SWE = 35 mm). Rainfall during the 2008 ice-free months was slightly above average (169 mm), followed by above-average snowfall during the ice-covered months 2008–2009 (SWE = 153 mm). Slightly above-average cumulative

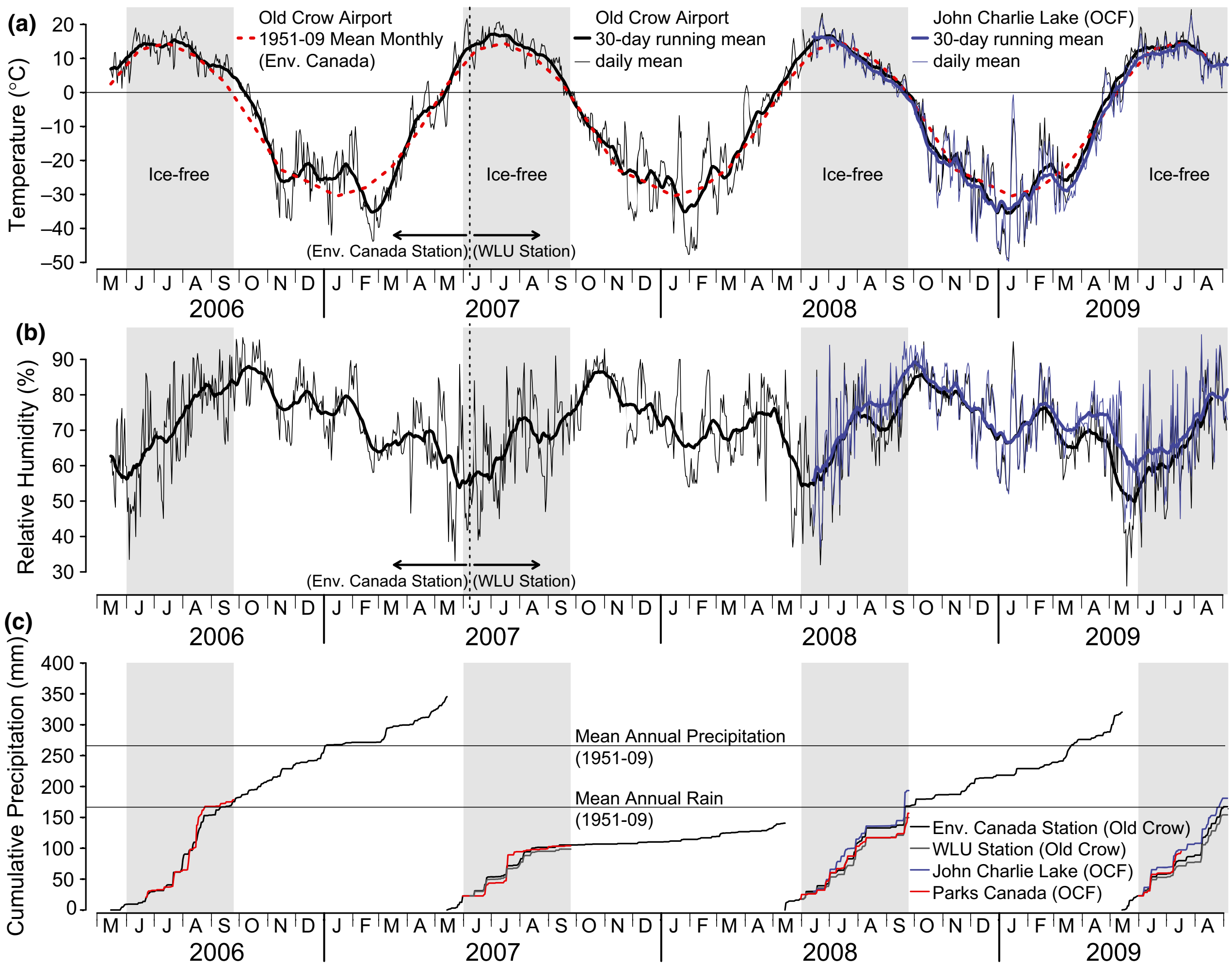

Fig. 3 Meteorological data collected between May 2006 and September 2009 at the Old Crow Airport, Old Crow, Yukon (from Environment Canada [2009] and WLU stations) and at John Charlie Lake in the central Old Crow Flats. Parameters include (a) temperature, (b) relative humidity and (c) cumulative precipitation. Mean daily data and 30-day running mean data were recorded by the Environment Canada station (1 June 2006–7 June 2007) and WLU station (8 June 2007–6 September 2009). Rainfall data were also recorded at the Parks Canada station.

rainfall (166 mm) occurred during the 2009 ice-free months prior to the final sampling campaign, with the most intense rain events occurring in August (e.g., 22 mm on 9 August). Overall, meteorological data indicate that June 2006–May 2007 (359.4 mm) and June 2008 – May 2009 (325.6 mm) were relatively wet, while June 2007–May 2008 (217.8 mm) was relatively dry in comparison to the long-term mean (Fig. 3c; 1953–2009 mean = 266 mm with confidence intervals ± 24.7 mm).

Land cover classification and lake catchment characteristics

A land cover classification was used to assess the proportion of land cover types in OCF including the catchments of the 57 study lakes. Woodland/forest vegetation, tall shrub vegetation, dwarf shrub/herbaceous vegetation, sparse vegetation and surface water account for 13%, 25%, 37%, 2%, and 23%, respectively, of the OCF (Fig. 4). Woodland/forest and tall shrub vegetation are more dominant along the southern and western portions of OCF, whereas dwarf shrub/herbaceous and sparse vegetation are more prominent in the central, northern, and eastern areas. For the headwaters of OCF located in the adjacent mountain ranges (total area = 13 923 km^2), land cover includes less tall shrub (18%) and surface water (10%), similar woodland/forest (15%) and greater proportions of dwarf shrub/herbaceous (51%) and sparse vegetation (7%). Occupying a total area of 1871 km^2, study-lake catchments, on average, are composed of 10% woodland/forest vegetation, 23% tall shrub vegetation, 48% dwarf shrub/herba-

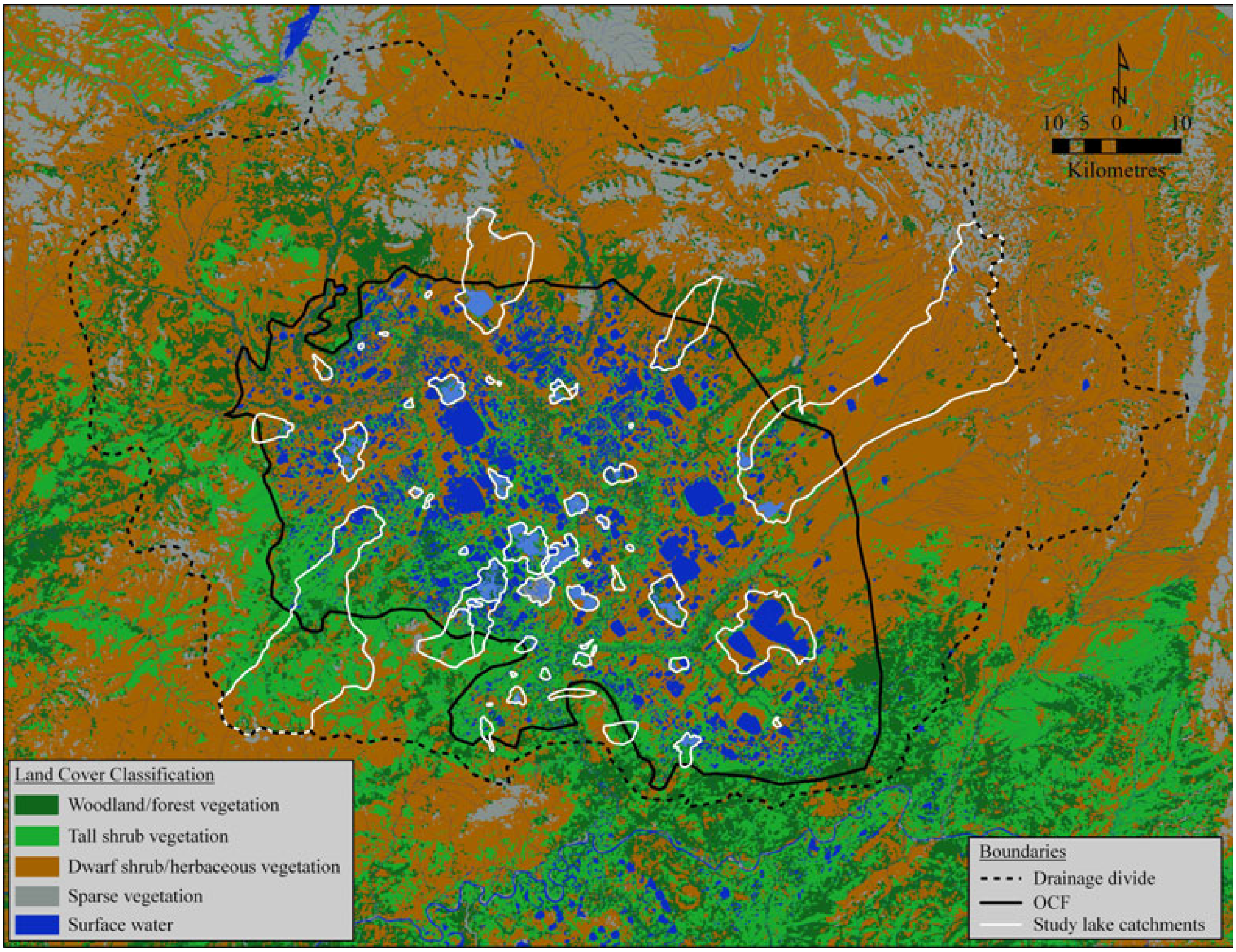

Fig. 4 Land cover map of the Old Crow Flats and surrounding watershed area. Study lake catchments are outlined in white.

ceous vegetation, 4% sparse vegetation and 15% surface water, comparable to the OCF landscape.

Lake surface areas (LA) and catchment areas (CA) were highly variable among sample sites, with values ranging from 0.002 to 13.209 km^2 (median = 0.286 km^2) and 0.209–660.384 km^2 (median = 4.957 km^2), respectively (Fig. 4). Smaller sized catchments tend to be located in central areas of OCF. Consequently, the LA/CA ratio is greater in these areas. Larger catchments generally occupy more peripheral portions of OCF, often including mountainous headwater areas. These catchments contain much less surface water and the LA/CA ratios are smaller than for more centrally located lakes.

Isotope hydrology

Lake hydrological conditions were assessed using a reference isotopic framework in conventional oxygen ($\delta^{18}O$) and hydrogen (δ^2H) space. The framework consists of two linear reference lines including the GMWL, which is defined by $\delta^2H = 8\delta^{18}O + 10$ (Craig, 1961) and the Local Evaporation Line (LEL; Fig. 5b and c). Extending to the right from the GMWL, the LEL generally has a slope of 4–6. This represents the expected trajectory in $\delta^{18}O$ – δ^2H space that local surface water isotopic compositions, fed by mean annual isotopic composition of precipitation (δ_P), undergo due to evaporation. An important reference point along the LEL is the isotopic composition of a terminal (i.e., closed-drainage) lake at isotopic and hydrological steady state, where evaporation equals inflow (δ_{SSL}). The isotopic composition of a lake approaching complete desiccation (δ^*) defines the terminus of the LEL. The relative importance of evaporation is positively correlated with lake water isotopic compositions along the LEL (i.e., relatively higher lake water compositions indicate greater evaporation relative to inflow). Lake water isotope compositions above or below the LEL can

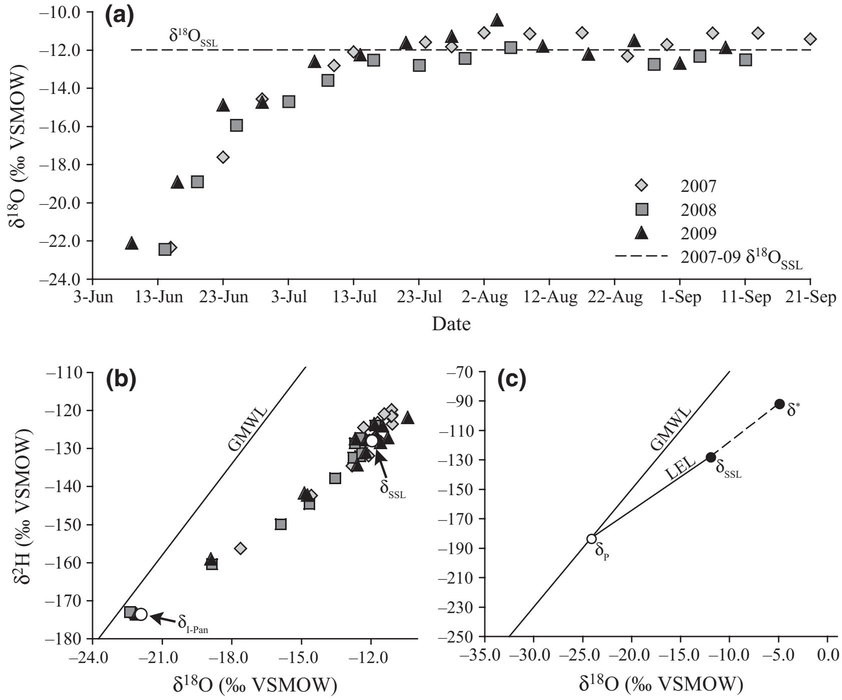

Fig. 5 (a, b) Isotope composition of water sampled from an evaporation pan maintained at the Old Crow airport from June to September for each year of the study (2007–2009). During each year, evaporation pan water reached isotopic steady-state, where inflow equals evaporation (δ_{SSL}), after 5 weeks of sampling and provides a robust reference point for development of the (c) Local Evaporation Line (LEL; $\delta^2H = 4.56\ \delta^{18}O–73.08$). The LEL was extended through the isotopic composition of pan source water ($\delta_{I\text{-}Pan}$) to the Global Meteoric Water Line (GMWL), the intersection of which represents the isotopic composition of mean annual precipitation (δ_P). The LEL extends to the calculated limiting isotopic composition for a lake approaching desiccation (δ^*; see Supporting Information).

be interpreted to reflect greater input of rain or snow than δ_P, respectively.

The isotopic composition of the source water for the evaporation pan ($\delta_{I\text{-}Pan}$) remained constant over the duration of the study ($\delta^{18}O = -21.9‰$, SD = 0.3‰; $\delta^2H = -173‰$ SD = 0.6‰; $n = 15$) and plotted close to the GMWL (Fig. 5b). For each year, $\delta^{18}O$ of water in the evaporation pan increased over five weeks before reaching isotopic steady state (2007 $\delta_{SSL} = -11.8‰$ for $\delta^{18}O$ and $-127‰$ for δ^2H, 2008 $\delta_{SSL} = -12.4‰$ for $\delta^{18}O$ and $-129‰$ for δ^2H, 2009 $\delta_{SSL} = -11.7‰$ for $\delta^{18}O$ and $-127‰$ for δ^2H). Given the consistency of δ_{SSL} among years, the three-year average δ_{SSL} ($\delta^{18}O = -12.0‰$, $\delta^2H = -128‰$) provides a robust reference point in $\delta^{18}O – \delta^2H$ space (Fig. 5c). Utilizing $\delta_{I\text{-}Pan}$ and δ_{SSL}, the LEL ($\delta^2H = 4.56\ \delta^{18}O–73.08$) for the three-year study period was constructed and extended to the GMWL, the intersection of which provides an estimate of the mean annual isotopic composition of precipitation ($\delta_P = -24.1‰$ for $\delta^{18}O$ and $-183‰$ for δ^2H; Table S1; Fig. 5c). Using the equation provided by Gonfiantini, 1986 (see Supporting Information), δ^* was found to vary by only 1.6‰ for $\delta^{18}O$ and 7‰ for δ^2H over the 3 years (Table S1). Given that δ^* and flux-weighted temperature and relative humidity values were generally similar over the three-year period (Table S1), a three-year average δ^* ($\delta^{18}O = -5.0‰$, $\delta^2H = -92‰$) value was used to define the δ_{SSL} - δ^* segment of the LEL (Table S1; Fig. 5c).

Lake water isotope compositions (δ_L) from each sampling interval were superimposed on the isotopic framework to identify seasonal and interannual patterns in hydrological conditions (Fig. 6). For each year, δ_L values plot along a strong linear trend (mean $r^2 = 0.97$) extending from the GMWL, at a slightly greater slope than the predicted LEL (2007: $\delta^2H = 5.30\ \delta^{18}O–59.6$, 2008: $\delta^2H = 5.40\ \delta^{18}O–59.0$, 2009: $\delta^2H = 5.19\ \delta^{18}O–62.3$). The sample set captured high variability in lake hydrological conditions as indicated by pronounced ranges in δ_L values for each sampling interval (Table S2). Overall, June values were more isotopically depleted while July and September values were relatively enriched. δ_L values from 2007 and 2009 showed a similar distribution on the isotopic framework (Fig. 6a and c). In contrast, δ_L values were positioned further along the LEL during 2008, with many lakes plotting close to or beyond δ_{SSL}, indicating greater evaporative isotopic enrichment (Fig. 6b). δ_L values had similar

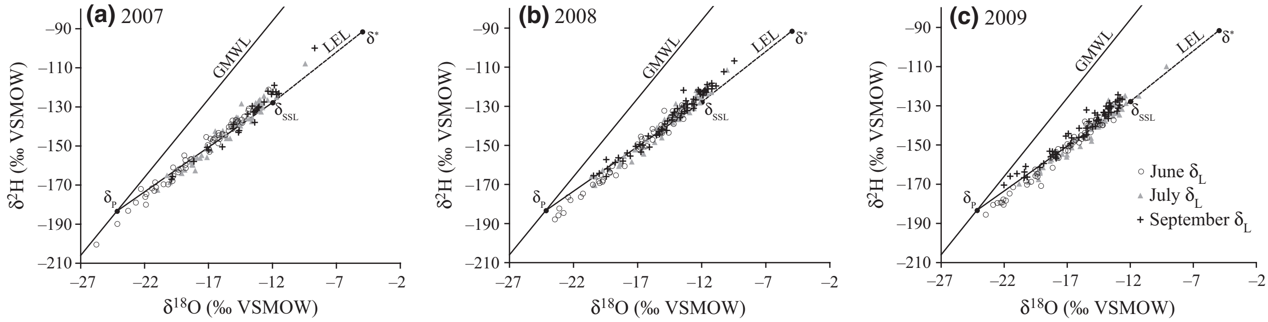

Fig. 6 Isotopic compositions of sampled lake water (δ_L) from each sampling campaign in (a) 2007, (b) 2008 and (c) 2009 superimposed on the isotopic framework (as presented in Fig. 5).

distributions above and below the LEL each year. δ_L values closer to the GMWL were typically positioned below the LEL reflecting a stronger influence of snowmelt (rather than rainfall) on water balances. Lakes with higher δ_L values showed greater influence from rainfall as indicated by values plotting above the LEL. The preferential influence of snowmelt on isotopically depleted lakes and rainfall on isotopically enriched lakes likely accounts for the apparent steeper slope of the δ_L values in comparison to the evaporation pan-derived LEL.

Lake-specific source water isotope compositions (δ_I) were calculated for each sampling interval to evaluate the relative roles of snowmelt vs. rain on lake hydrological conditions (Fig. 7). Scatterplots were sorted based on three-year mean July $\delta^{18}O_I$ rather than by the three-year mean ice-free season $\delta^{18}O_I$ to avoid including data from September 2007 when only 27 sites were sampled. During 2007–2009, lake-specific $\delta^{18}O_I$ values broadly ranged between −28.2‰ and −15.9‰. June had the greatest number of snowmelt-dominated lakes (i.e., $\delta^{18}O_I \leq \delta_P$) for each year (19, 30, 30 for 2007, 2008, and 2009, respectively; Table S2), reflecting the strong influence of snowmelt on lake water balances during the early ice-free season. The low number of snowmelt-dominated lakes in June 2007 is likely due to dilution from substantial rainfall in late summer 2006 and in spring 2007 shortly before sampling. While most lakes were rainfall-dominated (i.e., $\delta^{18}O_I > \delta_P$) later in the ice-free season, some lakes remained snowmelt-dominated (eight in 2007, 12 in 2008 and five in 2009; Table S2). Lakes whose δ_I values are close to δ_P (e.g., OCF26, OCF32, OCF7; Fig. 1) tended to oscillate frequently between snowmelt- and rainfall-dominated categories, reflecting the hydrological continuum that naturally exists among lakes in the data set. Indeed, OCF32 and OCF7 transitioned between categories in 2007 (Turner *et al.*, 2010), but seem more characteristic of lakes with snowmelt-dominated input waters based on the three-year data set. September 2009 had the greatest number of rainfall-dominated lakes (52; Table S2) following above-average August rainfall (Fig. 3c). Despite varying amounts of precipitation among years (Fig. 3c), there was little year-to-year difference in mean ice-free season δ_I values (Fig. 7b; Table S2).

Evaporation-to-inflow ratios (E/I) were calculated to evaluate the importance of lake vapor loss for each sampling interval. Scatterplots of E/I ratios organized by the gradient of three-year mean July $\delta^{18}O_I$ values clearly demonstrate that lakes fed predominantly by snowmelt tend to undergo less evaporative enrichment than lakes fed more by rainfall (Fig. 8). Based on this relationship, the categorization of lakes was further refined by adjusting slightly the threshold separating snowmelt- and rainfall-dominated lakes by +0.1% (to -24.0% for $\delta^{18}O$) so that the hydrological conditions of OCF32 and OCF7, including low E/I ratios and variability, are more appropriately categorized as snowmelt-dominated. E/I ratios for all lakes were consistently low during each spring (2007–2009 June mean E/I = 0.33; Fig. 8a) and generally increased during the early ice-free season (2007–2009 July mean E/I = 0.52; Fig. 8a). On average, E/I ratios remained comparable between middle and late ice-free season (2007–2009 September mean E/I = 0.53). Results from September 2009 deviate from this seasonal pattern as most E/I ratios (mean E/I = 0.34) were less than in July 2009 (mean E/I = 0.47; Table S2) due to substantial rainfall in August of 2009 (Fig. 3c). There were clear interannual differences in E/I values during 2007–2009 (Fig. 8b). E/I ratios were lower during 2009 (mean E/I = 0.37) than during 2007 (mean E/I = 0.41) and 2008 (mean E/I = 0.57; Fig. 8b). E/I values were the lowest during the wet spring conditions of June 2007 and 2009 (mean E/I = 0.28 and 0.31, respectively; Table S2). In contrast, E/I values were higher in June 2008 (mean E/I = 0.42; Table S2) than spring of other sampling years when much less precipitation occurred prior to sampling (Fig. 3c). This pattern continued in 2008, with mid- and late-summer E/I values (July mean E/I = 0.63,

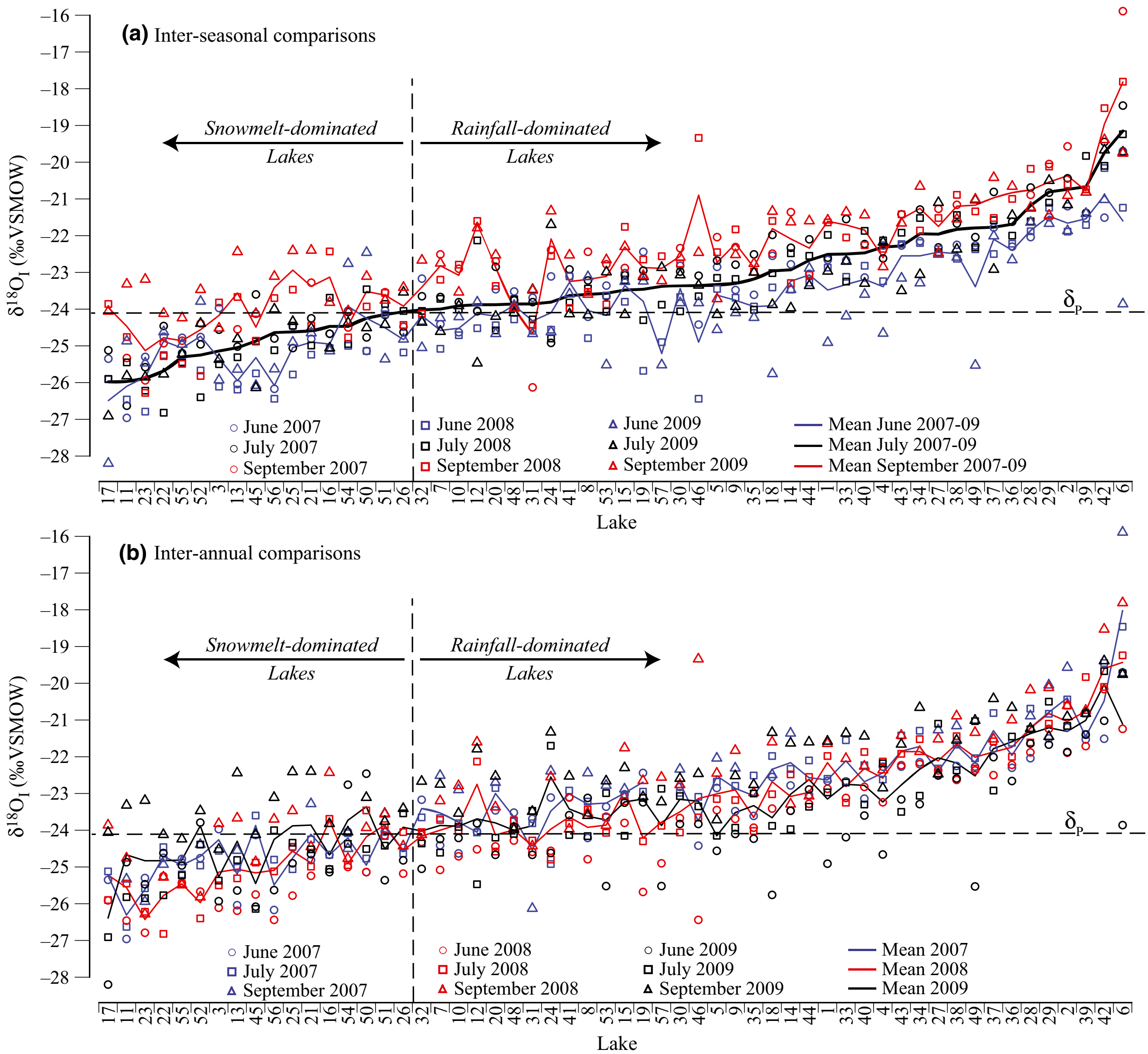

Fig. 7 Isotopic compositions of lake-specific input water ($\delta^{18}O_I$; see Supporting Information) over (a) seasonal and (b) interannual time scales. Lakes are arranged from lowest to highest, according to their three-year mean July $\delta^{18}O_I$ values. Solid lines in panel (a) represent mean $\delta^{18}O_I$ values calculated for each lake for the early (blue), mid- (black) and late (red) ice-free seasons. Solid lines in panel (b) represent mean $\delta^{18}O_I$ values calculated for each lake for 2007 (blue), 2008 (red) and 2009 (black) ice-free seasons. Separation of snowmelt- ($\delta^{18}O_I \leq -24.1$‰) from rainfall-dominated lakes ($\delta^{18}O_I > -24.1$‰) is represented by the vertical dotted line.

September mean E/I = 0.65) that were higher than any other sampling campaign. The majority of snowmelt-dominated lakes had lower E/I values and experienced less variability among years than rainfall-dominated lakes (mean snowmelt-dominated lakes 2007–2009 E/I = 0.28, SD = 0.06; mean rainfall-dominated lakes 2007–2009 E/I = 0.55, SD = 0.14; Fig. 8b). Using a threshold E/I value of 0.5 (i.e., 50% evaporative water loss), 30 lakes experienced evaporation-dominated hydrology prior to at least one of the sampling episodes in 2007, 40 in 2008 and 23 in 2009. All but two of these lakes are a subset of the rainfall-dominated category.

There are exceptions to these general patterns, which highlight lake- and catchment-specific geomorphological, physiographic, and land-cover characteristics that influence hydrological conditions. For example, the four lakes in the snowmelt-dominated category with the lowest δ_I values have relatively high and seasonally variable E/I values, though not as high and variable on average as lakes in the rainfall-dominated category.

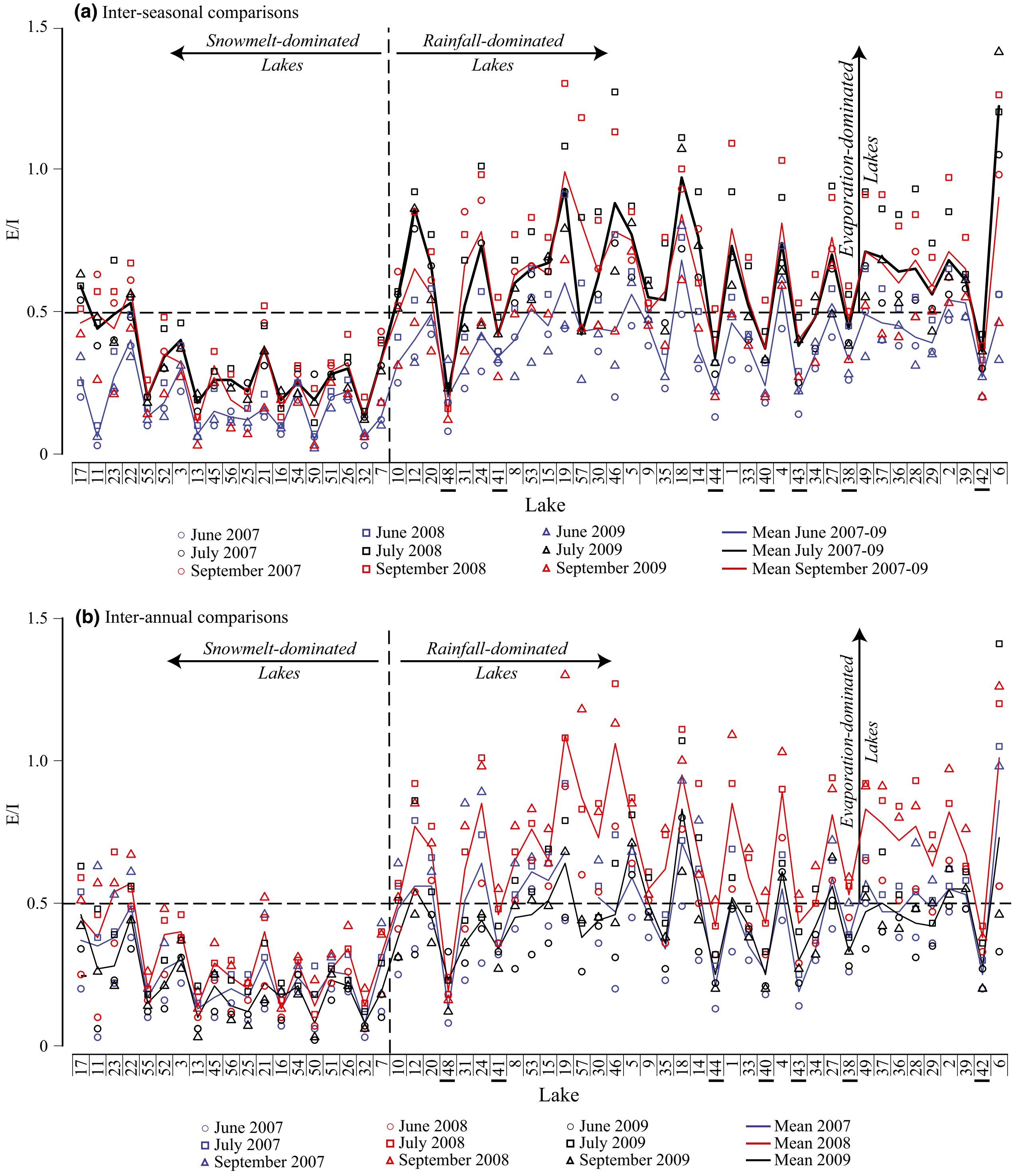

Fig. 8 (a) Evaporation to inflow ratios (E/I; see Supporting Information) over (a) seasonal and (b) interannual time scales. Lakes are arranged, from lowest to highest, according to their three-year mean July $\delta^{18}O_I$ values. Solid lines in panel a) represent mean E/I values calculated for each lake for the early (blue), mid- (black), and late (red) ice-free seasons. Solid lines in panel b) represent mean E/I values calculated for each lake for 2007 (blue), 2008 (red) and 2009 (black) ice-free seasons. Lakes with E/I > 0.5 are evaporation-dominated. Underscored lake numbers identify exceptions discussed in the text. Lakes OCF32 and OCF7 were re-classified as snowmelt-dominated based on their δ_I values and low E/I ratios.

Field observations suggest that this is attributable to less hydrological connectivity later in the ice-free season compared to other snowmelt-dominated lakes. In addition, some rainfall-dominated lakes had relatively low E/I ratios (i.e., OCF38, OCF40–44). These lakes are located along the east to north OCF periphery and likely experienced greater inflow from upstream locations relative to other rainfall-dominated lakes. Notably, OCF42 had the second highest δ_I values (i.e., rainfall-dominated) but low E/I ratios because it transfers abundant through-flow from two large rainfall-dominated lakes that typically remain ice-covered later in the season (mid to late June, 2–3 weeks after all other study lakes are ice-free; Geldsetzer *et al*., 2010) and hence undergo limited evaporative enrichment. Also classified as a rainfall-dominated lake, OCF48 experienced consistently low E/I ratios due to inflow of shallow groundwater from a neighboring forested upland (Timber Hill) (MacDonald *et al*., 2012). Thus, the hydrological behavior of OCF42 and OCF48 are analogous to the greater hydrological connectivity of the majority of snowmelt-dominated lakes. Although not shown in Figs 7 and 8, OCF47 is a striking anomaly for a lake within the snowmelt-dominated category. This lake exhibited relatively high E/I values in July (mean July 2007–2009 E/I = 0.78) and on the basis of field observations, we attributed to a 'chain of lakes effect' (Gat & Bowser, 1991). OCF47 was not included in further analysis since it receives pre-evaporatively enriched inflow across a beaver dam that retains catchment inflow in the larger lake upstream. It is likely that the true δ_I values for this site were offset from the GMWL, which resulted in an overestimation of E/I.

Spatial autocorrelation among δ_I and E/I values was assessed using Moran's *I* coefficients and contour maps were created to identify spatial patterns in these isotope-inferred metrics over seasonal- and interannual timescales (Fig. 9). Moran's *I* coefficients calculated for δ_I and E/I values during each sampling interval show moderate spatial association, with values ranging from 0.16 to 0.37. δ_I values were interpolated to identify areas where lakes were snowmelt-dominated or rainfall-dominated for each sampling interval (Fig. 9a). Snowmelt-dominated lakes in June were concentrated in more peripheral areas of OCF including south, west, and north-central sub-regions. As rainfall was the primary precipitation type during the ice-free seasons, the number and spatial extent of snowmelt-dominated lakes decreased and many lakes became rainfall dominated. Seasonal patterns of δ_I spatial distributions were consistent among years despite highly variable interannual precipitation amounts.

Contour maps of E/I values show seasonal patterns that have similarities and differences among years (Fig. 9b). The spatial distribution of E/I values in June was typically less variable among lakes, especially during the wet spring of 2007, compared to later in the ice-free season. Lakes located in the central OCF generally experienced greater increases in E/I values compared to lakes in peripheral areas in July 2007–2009 and September 2008. The greatest spatial variability in E/I values occurred in September 2008 when many lakes were evaporation-dominated in the central and northwestern areas of OCF. In contrast, E/I values in September 2009 decreased following intense August rainfall and their spatial distribution closely resembles the June 2009 E/I map. Unlike δ_I, the spatial distribution of E/I values were seasonally variable in response to precipitation amounts.

Relations among climate, land cover and lake hydrological categories

Principal components analysis ordination identifies that a strong association exists between catchment land-cover type and lake hydrological categories (Fig. 10a). The first (λ_1 = 0.33) and second (λ_2 = 0.28) axes of the PCA ordination of the 56 (not including OCF47–see above) study lakes indicate that the percentages of the five land-cover classes explained a large proportion (61%) of the variation in catchment characteristics among lakes. Axis 1 separated catchments mainly based on proportion (%) of tall shrub and dwarf shrub/herbaceous land-cover types. Specifically, catchments with higher % dwarf shrub/herbaceous vegetation were positioned to the left along axis 1, whereas catchments with lower values of this variable were positioned to the right and were associated with higher % tall shrub vegetation. In contrast, axis 2 separated catchments based primarily on % surface water, % sparse vegetation and % woodland/forest vegetation. Catchments with high % surface water were positioned mainly within the central and upper left areas of the plot, whereas catchments with less surface water and more % woodland/forest vegetation were positioned low along axis 2. The different symbols of the sample scores coded the lakes as snowmelt- or rainfall-dominated based on mean July δ_I values (2007–2009). Sample scores are also distinguished by mean July E/I ratios (2007–2009). Important patterns that emerge include the association of snowmelt-dominated lakes, which typically have low E/I ratios (≤0.5), with catchments containing a relatively higher percent cover of woodland/forest and tall shrub vegetation. In contrast, catchments of most rainfall-dominated lakes, which typically possess higher E/I ratios than snowmelt-dominated lakes, tend to be covered by dwarf shrub/herbaceous vegetation and surface water. Notably, lakes having the

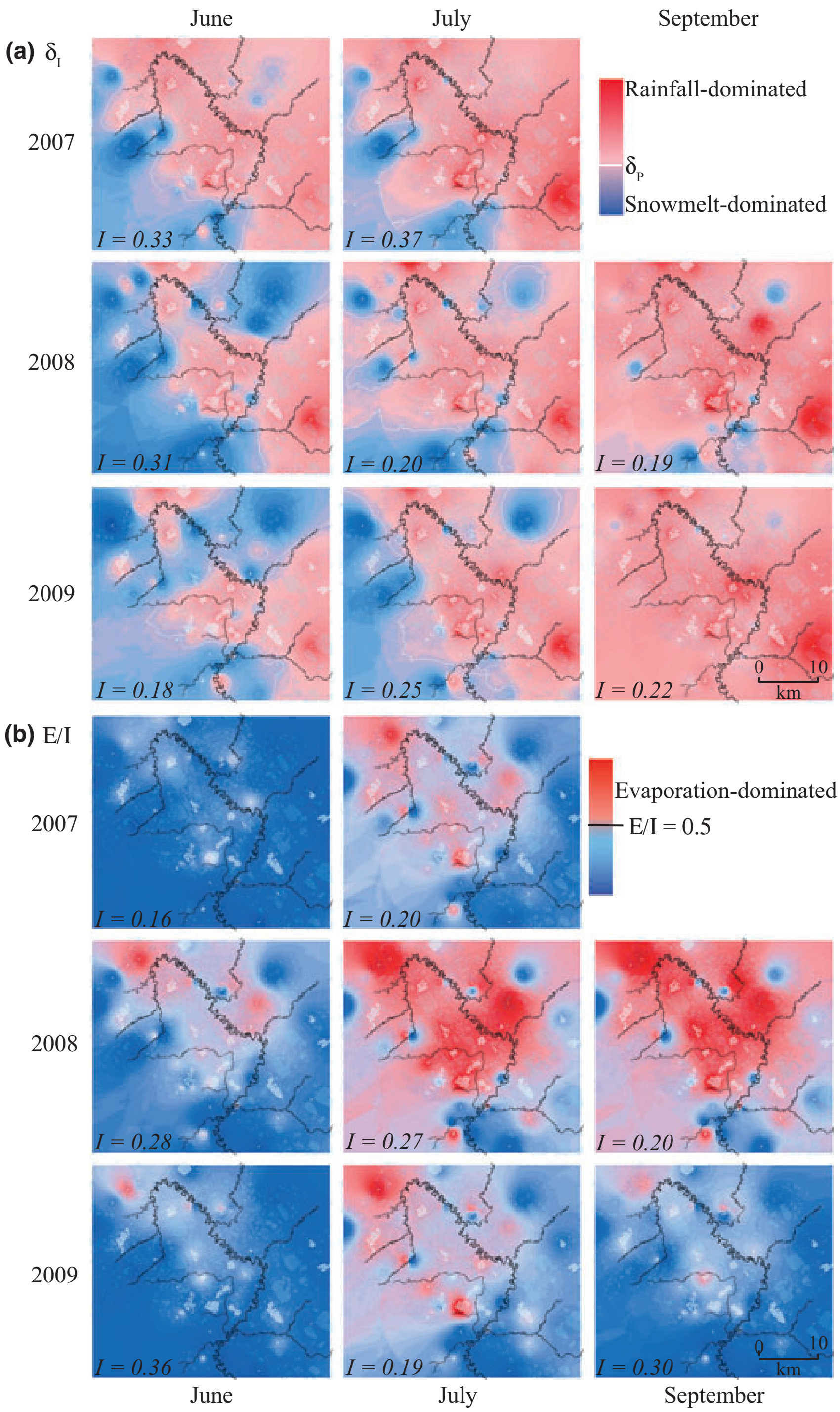

Fig. 9 Spatial distributions for (a) $\delta^{18}O_I$ and (b) E/I values during each sampling interval (2007–2009), as determined using inverse distance-weighted interpolation methods. September 2007 maps are not included since insufficient data were available for interpolation due to unfavorable sampling conditions. Moran's *I* coefficients represent the level of spatial autocorrelation (Anselin, 1995) and are listed in the bottom left of each map.

highest E/I values (>0.8) all cluster along the left side of the PCA (with high % dwarf shrub/herbaceous vegetation and % surface water).

The above relations are summarized quantitatively in Fig. 10b, which illustrates the average catchment land cover characteristics for lakes of each hydrological

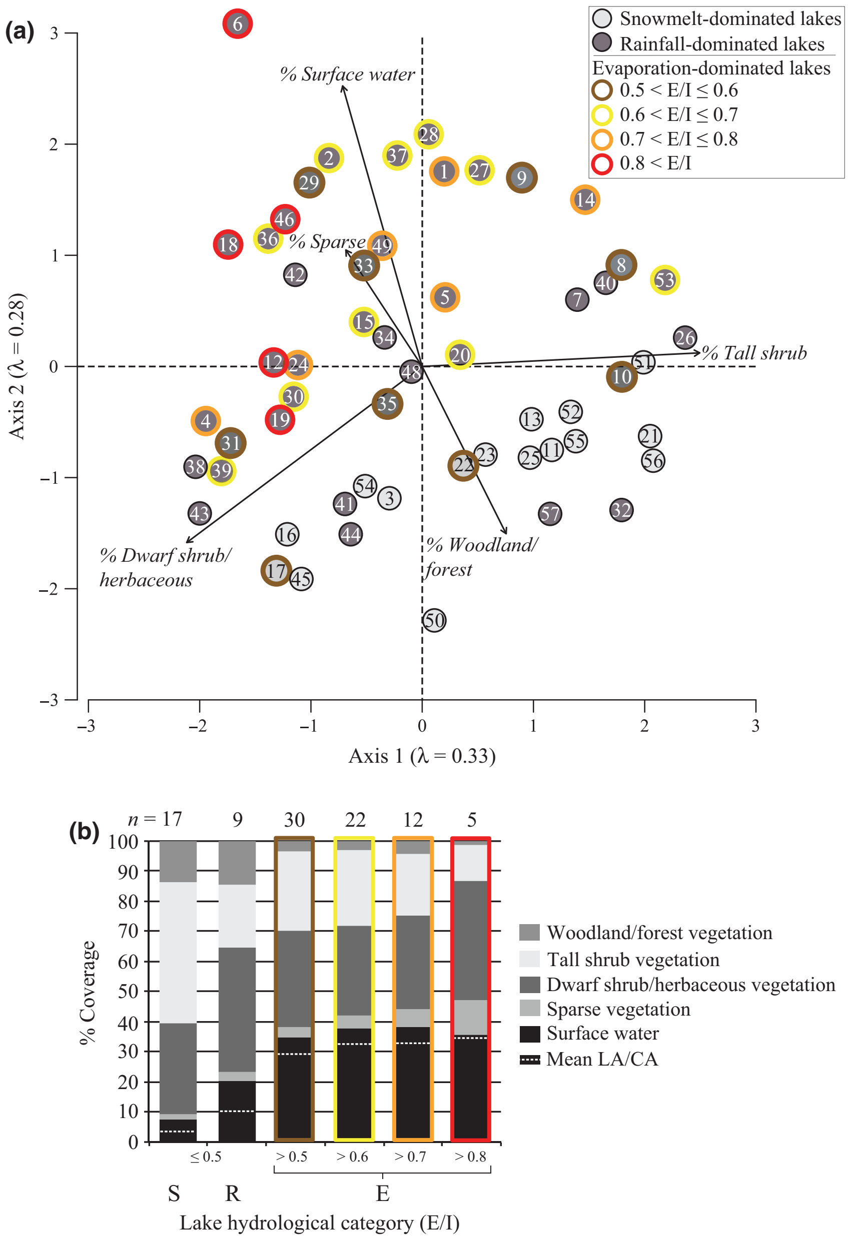

Fig. 10 (a) Principal components analysis showing variation among the 56 (OCF47 was removed – see text) study lakes in relative abundance (%) of the five main land-cover types in their catchments. To explore relations between land-cover characteristics and lake hydrology, the sample scores were coded according to their hydrological lake category (snowmelt-, rainfall-, or evaporation-dominated) based on mean (2007–2009) July δ_I and E/I values. Vectors for catchment characteristics were expanded fourfold to span the range of sample scores. (b) Average catchment characteristics among lakes for each hydrological category (i.e., snowmelt-dominated [S], low evaporation-influenced rainfall-dominated [R] and evaporation-dominated [E]). Note that for snowmelt- and rainfall-dominated lakes, only those with mean July E/I ≤ 0.5 are included; evaporation-dominated lakes are grouped based on mean July E/I > 0.5, 0.6, 0.7, and 0.8.

category. This figure shows how catchment land-cover characteristics differ between snowmelt-dominated lakes and (low evaporation-influenced) rainfall-dominated lakes having a mean July E/I ≤ 0.5, as well as subsets of rainfall-dominated (mean July E/I > 0.5, 0.6, 0.7, 0.8), which we classify here as evaporation-dominated. The most salient feature of this synthesis is that lake hydrology varies systematically with the structure and aerial proportion of catchment land cover. Catchments of snowmelt-dominated lakes, which are most prevalent in southern and western locations of OCF, are covered in relatively high proportions of woodland/forest and tall shrub vegetation (combined mean = 60%) and lower proportions of dwarf shrub/herbaceous and sparse vegetation, and surface water (combined mean = 40%). On average, snowmelt-dominated lakes only occupy 4% of their total catchment area (i.e., LA/CA). Catchments of low-evaporation lakes with rainfall-dominated hydrology, most of which are located in more central areas of OCF, have lower proportions of woodland/forest and tall shrub vegetation (combined mean = 35%) and higher proportions of dwarf shrub/herbaceous and sparse vegetation and surface water (combined mean = 65%). Low evaporation-influenced rainfall-dominated lakes tend to possess higher LA/CA ratios (mean = 10%) than snowmelt-dominated lakes (4%). Evaporation-dominated lakes have substantially higher mean LA/CA (29%). The catchments for these lakes are also distinguished by greater surface water (35%) compared to low evaporation-influenced rainfall-dominated lakes (20%) and snowmelt-dominated lakes (8%). For evaporation-dominated lakes where $E/I > 0.8$, catchments consist mainly of dwarf shrub/herbaceous vegetation and surface water (combined mean = 76%).

An ANOSIM test showed that catchment landcover exhibited moderate variation (global $R = 0.42$; $P = 0.00001$) according to lake hydrological categories [snowmelt-dominated ($E/I \leq 0.5$), low evaporation-influenced rainfall-dominated ($E/I \leq 0.5$), and evaporation-dominated ($E/I > 0.5$)]. Pairwise test results indicate that the differences in catchments of snowmelt-dominated ($n = 17$) and evaporation-dominated ($n = 30$) lakes are greater ($R = 0.51$; $P = 0.00001$) than those between low evaporation-influenced rainfall-dominated ($n = 9$) and evaporation-dominated lakes ($R = 0.33$; $P = 0.003$). Land-cover characteristics also showed variation to a lesser degree between snowmelt-dominated and low evaporation-influenced rainfall-dominated lakes ($R = 0.26$; $P = 0.008$). Land-cover characteristics did not differ significantly among the four subgroups of evaporation-dominated lakes ($E/I > 0.5$, 0.6, 0.7 and 0.8; all $R < 0.1$, and $P > 0.17$). Land cover differences in evaporation-dominated lakes with $E/I > 0.8$ may not be detectable by the ANOSIM test because of the small number of lakes in this group ($n = 5$).

Discussion

Quantitative relations between catchment land-cover characteristics and lake hydrology substantially refines our previous observations (Turner *et al.*, 2010) and are consistent with results from other studies. Within areas of taller and denser vegetation (e.g., spruce and willow forest), snow is more effectively intercepted and accumulates greater snowpack volume than in areas of low (i.e., tundra) vegetation, as noted in other studies (Pomeroy *et al.*, 1997; Liston & Sturm, 1998; McFadden *et al.*, 2001; Sturm *et al.*, 2001; Brock *et al.*, 2009). Lakes situated in catchments with relatively larger proportions of woodland/forest and tall shrub vegetation (ca. 60%) appear to receive greater inflow during spring melt following winters characterized by both high and low snowfall. As a result of abundant snow capture in these catchments, snowmelt-dominated lakes typically possess low E/I values, even during extended dry weather in 2008. Many of these catchments also have mountainous headwaters that generate slope runoff. We further recognized that some snowmelt-dominated lakes having relatively high and variable E/I values are attributable to a reduction in hydrological connectivity later in the ice-free season based on examination of oblique aerial photographs. In contrast to snowmelt-dominated lakes, catchments that have higher proportions of dwarf shrub/herbaceous and sparse vegetation, and surface water (ca. 60%) typically contain low evaporation-influenced rainfall-dominated lakes and likely experience greater loss of snow during winter than snowmelt-dominated lake catchments due to redistribution by predominant northeasterly winds (Turner *et al.*, 2010). As a result, these lakes receive proportionately less snowmelt inflow and are more susceptible to becoming evaporation-dominated later in the ice-free season (Fig. 9b). Notably, our analysis suggests that lakes whose catchments contain at least 75% combined dwarf shrub/herbaceous vegetation and surface water appear to be most vulnerable to evaporative lake-level drawdown. Further studies to identify hydrological conditions of other lakes with these catchment land-cover characteristics are needed to test this notion.

Conducting this study over 3 years provided the opportunity to examine the additional effects of widely varying precipitation on lake hydrology. Results indicate that the hydrological responses to varying precipitation were clearly more pronounced for rainfall-dominated and especially for the subset of evaporation-dominated lakes than for snowmelt-dominated lakes. For example, E/I values of rainfall-dominated and evaporation-dominated lakes varied substantially among years in concert with interannual variations in cumulative precipitation, indicating that this is a key driver of hydrological variability for these lake types. E/I values of rainfall-dominated and evaporation-dominated lakes were low during the wet years of 2007 and 2009, while E/I values were high during the dry year of 2008. Conversely, the E/I ratios of snowmelt-dominated lakes were less affected by interannual differences in cumulative precipitation because contributions of snowmelt were sufficient to offset evaporation even during the low-snowfall winter that preceded the 2008 ice-free season. These results reveal clear relations among climate, catchment characteristics (i.e., the composition and structure of catchment land cover) and hydrology, which inform how these lakes are likely to respond to future climate and environmental change.

Anticipating future hydrological change

In recent decades, northern regions have experienced more rapid increases in air temperature than other regions of the Earth (ACIA, 2004). According to dendroclimatological analyses, OCF is presently warmer than it has been during any other interval of the past ca. 300 years (Porter & Pisaric, 2011). Mean annual air temperature is predicted to continue to increase by 4–5 °C in Arctic regions during the next century (Kattsov *et al.*, 2005). Precipitation is expected to increase by 7.5–18% (Kattsov *et al.*, 2005), although model results vary substantially within and among regions (Prowse *et al.*, 2006). Notably, climate models for the 21st century suggest that high-latitude regions, including the northern Yukon, may experience increasing snowfall on the order of 10 cm yr^{-1} decade^{-1} (Krasting *et al.*, 2013). In response, it is expected that widespread hydrological changes will occur in northern lake-rich landscapes. For example, as a consequence of increased temperature and longer ice-free seasons, it has been predicted that there will be an increase in evaporative drawdown of lakes (Schindler & Smol, 2006), possibly leading to widespread desiccation as observed recently in Canada's High Arctic (Smol & Douglas, 2007). Carroll *et al.* (2011) identified a net reduction of >6700 km^2 in the surface area of lakes across northern Canada during the past decade, which they attributed to increased evaporation. With permafrost thaw, water loss from thermokarst lakes may also increase as a result of vertical drainage (Yoshikawa & Hinzman, 2003; Smith *et al.*, 2005; Riordan *et al.*, 2006), although this effect is dependent on the permeability of underlying sediments (Jepsen *et al.*, 2013). Increased precipitation and lateral hydrological connectivity associated with accelerated permafrost thaw may offset lake water loss by evaporation or drainage (Avis *et al.*, 2011). Indeed, a recent study illustrated widely differing hydrological responses of neighboring shallow tundra ponds in the western Hudson Bay Lowlands to 20th century climate change, which was linked to differences in hydrological connectivity of the basins (Wolfe *et al.*, 2011b). Here too, we have identified the importance of hydrological connectivity as a feature influencing the water balances of lakes within our snowmelt-dominated category. Carroll *et al.* (2011) and Avis *et al.* (2011) also recognized that local variability likely contributes to observed and anticipated hydrological changes. Although this insight is challenging to attain at the landscape scale, determining the relative importance of drivers is key for predicting future hydrological conditions in northern lake-rich regions.

As demonstrated here, interactions between catchment land-cover characteristics and meteorological conditions generate variability and diversity in lake hydrological conditions in OCF. Identifying these linkages provides insight into important drivers of local hydrological complexity that defines this and possibly other northern lake-rich landscapes. This information is critical for anticipating how lake hydrological conditions are likely to respond to changing climate and land cover characteristics, as schematically illustrated for OCF in Fig. 11. Overall, lakes in OCF are unlikely to follow a single hydrological trajectory. Rather, as climate continues to change, multiple hydrological outcomes are probable. As further elaborated below, hydrological responses can be expected to be individualistic among lakes and dependent on the moisture

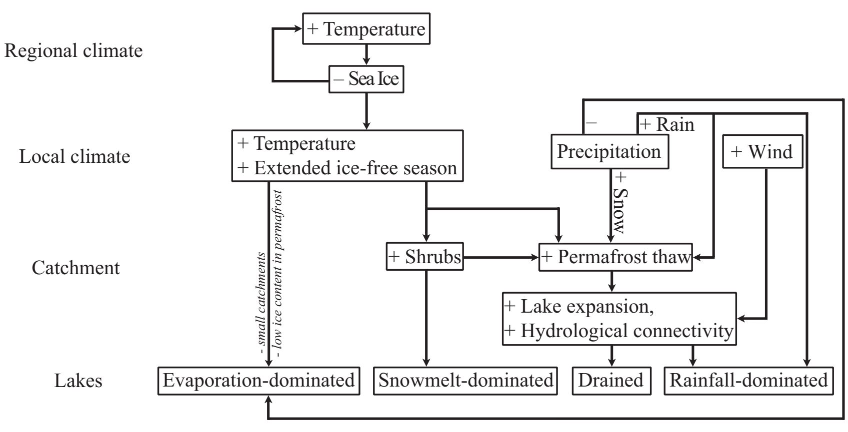

Fig. 11 Schematic flow chart identifying potential linkages among climate conditions, catchment land-cover characteristics, and hydrological conditions in northern thermokarst lake-rich environments, such as OCF.

regime, changes in catchment characteristics (land cover) and permafrost conditions.

Similar to other studies of thermokarst lakes (e.g., Jones *et al*., 2009), our analysis identified that precipitation was a key driver of interannual variability in hydrological conditions. This was especially apparent for rainfall-dominated and the subset of evaporation-dominated lakes. The hydrological conditions of snowmelt-dominated lakes were much more consistent among years despite varying interannual precipitation. The relative importance of snowmelt vs. rainfall was strongly associated with catchment characteristics (i.e., land cover and physiography). In the event of reduced precipitation and increasing evaporation, the latter possibly driven by a longer ice-free season, lake hydrological conditions will likely continue to be strongly influenced by snowmelt for lakes within catchments containing high proportions of woodland/forest and tall shrub vegetation that effectively capture snow drifts. In contrast, lakes with catchments dominated by dwarf shrub/herbaceous vegetation, sparse vegetation and surface water are most susceptible to becoming evaporation-dominated. Increased evaporative water loss may be offset by the meltwater from snow captured by increased shrub growth (in response to lengthened growing seasons), which has been observed along latitudinal tundra-taiga transition zones (Myers-Smith *et al*., 2011; Lantz *et al*., 2013) and in field experiments (Chapin *et al*., 1995; Hobbie & Chapin, 1998; Hudson *et al*., 2011), and has been linked with loss of multi-year sea ice in the Arctic Ocean (e.g., Beaufort Sea; Bhatt *et al*., 2010). Local elders and land users have also observed increased shrub coverage in OCF (ABEK Co-op, 2007). As a result, a transition from rainfall- to snowmelt-dominated hydrology (and more positive water balances) may be occurring in lakes that are surrounded by catchments large enough to generate sufficient snowmelt runoff (Fig. 11). Lakes that currently become evaporation-dominated during low-precipitation years (as in 2008) will likely experience a higher frequency of evaporation-dominated hydrological conditions, since they are typically situated in small catchments that are unlikely to generate sufficient snowmelt runoff, even with increased shrub growth.

Hydrological responses of lakes in thermokarst landscapes to climate change are also governed by permafrost conditions. Although we have no measurements of lake taliks, ground temperatures or permafrost thickness in the catchments of our 57-lake study set, the literature affords opportunity to anticipate the role of changes in permafrost on the hydrological conditions of lakes in OCF. Clearly, permafrost is expected to thaw due to increasing atmospheric temperature (Osterkamp & Romanovsky, 1999; Burn & Kokelj, 2009). While observed vertical drainage of lakes elsewhere has been linked with warming conditions (Yoshikawa & Hinzman, 2003), this process is likely inhibited in OCF since lakes are underlain by glaciolacustrine clay. However, ground temperature changes surrounding lakes in response to increased snowpack and rainfall (or increased seasonal frequency of intense rainfall events) and increased atmospheric temperature may have considerable hydrological implications. For example, these factors often lead to surface water ponding, increased hydrological connectivity and lake expansion (Fig. 11; Brewer *et al*., 1993; Marsh & Neumann, 2001; Payette *et al*., 2004; Jorgenson *et al*., 2006; Jones *et al*., 2011).

Lake expansion and catchment surface water accumulation may lead to a range of hydrological outcomes depending on rate of lake expansion, subsequent changes in catchment land cover (i.e., terrestrial to surface water) and proximity to lower lying areas. For example, if lakes experience significant expansion and coalescence over a long period, widespread drowning of snow-capturing forest/woodland and shrub vegetation may induce a hydrological transition to rainfall-dominated conditions, and possibly, make lakes more susceptible to the effects of evaporation. Alternatively, accelerated thermokarst processes and lake expansion may lead to an increase in frequency of lateral drainage events (Fig. 11; Prowse *et al*., 2006; Jones *et al*., 2011). If in close proximity to lower lying areas or an ice-wedge complex, expanding lakes may be more susceptible to drainage due to overflow or erosion along surrounding ice-wedges (Mackay, 1988; Brewer *et al*., 1993; Marsh & Neumann, 2001), possibly triggered by intense snow melt and rainfall events. This appears to have been the case for Zelma Lake, one of the largest lakes in OCF, which drained in June 2007 (Turner *et al*., 2010). Wet conditions were likely also the trigger for drainage of OCF48 in the late-1980s, as determined using paleolimnological methods (e.g., MacDonald *et al*., 2012). After drainage, permafrost aggradation initiates (as early as the following winter) (Mackay, 1999), and it can be expected that the water levels of remnant ponds will become increasingly responsive to precipitation owing to larger terrestrial catchments (Roach *et al*., 2011) and changing land cover (i.e., increased shrub growth within the drained lakebed; Fig. 11).

Lake shorelines in OCF experiencing the most rapid rates of expansion are located in areas dominated by tundra (e.g., dwarf shrub/herbaceous) vegetation, high ground-ice content, and where fetch and lake orientation result in aggressive wave action and spring ice-push (Roy-Léveillée & Burn, 2010). An increase in prevailing wind velocity or frequency of high winds may accelerate this process (Fig. 11). Wind is a less influential driver of receding shorelines in forested areas, although lakes do expand in these areas as a result of thermal erosion (Roy-Léveillée & Burn, 2010).

Concluding remarks

Combining quantitative analysis of water isotope tracer data and remote sensing imagery is a novel research approach that we demonstrate to be highly informative for hydrological characterization of lakes in OCF. Findings revealed that hydrological lake categories are associated with land cover features and physiographic location – aspects that are difficult to account for in studies solely reliant on remote sensing imagery (e.g., Carroll *et al*., 2011). Given that catchment land-cover characteristics in northern lake-rich landscapes are often dynamic and responsive to changes in climate, lakes are likely to follow multiple hydrological trajectories over time. For local managers (Vuntut Gwitchin Government and Parks Canada), knowledge of diverse hydrological outcomes over broad spatial scales may also be useful for informing a vulnerability assessment of water resources in OCF. Our integrative approach provides a new opportunity to evaluate processes responsible for hydrological changes in other northern lake-rich regions, identified as leading-edge Arctic landscapes in transition (Rowland *et al*., 2010).

Acknowledgements

We thank the community members of Old Crow who have shared knowledge of Old Crow Flats that has informed our research and who have provided logistical support in the field including Danny Kassi, James Itse, Erika Tizya-Tramm, Robert Bruce, Shaun Bruce, Renee Charlie, Dennis Frost, Shel Graupe and Jennifer Lee. Ann Balasubramaniam, Jana Tondu, Lauren MacDonald, Nicholas Sidhu, Matt Ennis and Alex MacLean also assisted with field work. Precipitation data from the meteorological station in Vuntut National Park were provided by Ian McDonald of Parks Canada. We thank the staff of the UW-EIL for isotope analyses. Funding for this research was provided by the Government of Canada International Polar Year Program, the Natural Sciences and Engineering Research Council of Canada Northern Research Chair Program, the Polar Continental Shelf Program of Natural Resources Canada, the Northern Scientific Training Program of Aboriginal Affairs and Northern Development Canada, Natural Sciences and Engineering Research Council of Canada Postgraduate Scholarship, W. Garfield Weston Foundation Northern Research Award and Ontario Graduate Scholarships.

References

ABEK Co-op (2007) Arctic Borderlands Ecological Knowledge Co-operative. Community Reports 2005-2006. Available at: http://www.taiga.net/coop/community/index.html (accessed 16 February 2010).

ACIA (2004) *Impacts of a Warming Arctic: Arctic Climate Impact Assessment*. Cambridge University Press, Cambridge.

Anselin L (1995) Local indicators of spatial association—LISA. *Geographical analysis*, **27**, 93–115.

Avis CA, Weaver AJ, Meissner KJ (2011) Reduction in areal extent of high-latitude wetlands in response to permafrost thaw. *Nature Geoscience*, **4**, 1–5.

Bhatt US, Walker DA, Raynolds MK *et al*. (2010) Circumpolar Arctic tundra vegetation change is linked to sea ice decline. *Earth Interactions*, **14**, 1–20.

Brewer M, Carter LD, Glenn R, Murray DF (1993) Sudden drainage of a thaw lake on the Alaskan Arctic coastal plain. *Proceedings of Sixth International Conference on Permafrost, Beijing, China*, Vol 1, pp. 48–53. South China University of Technology Press, Guangzhou, China.

Brock BE, Yi Y, Clogg-Wright KP, Edwards TWD, Wolfe BB (2009) Multi-year landscape-scale assessment of lakewater balances in the Slave River Delta, NWT, using water isotope tracers. *Journal of Hydrology*, **379**, 81–91.

Burn CR, Kokelj SV (2009) The environment and permafrost of the Mackenzie Delta Area. *Permafrost and Periglacial Processes*, **20**, 83–105.

Carroll ML, Townshend JRG, DiMiceli CM *et al*. (2011) Shrinking lakes of the Arctic: spatial relationships and trajectory of change. *Geophysical Research Letters*, **38**, L20406.

Chapin FS III, Shaver GR, Giblin AE *et al*. (1995) Responses of Arctic tundra to experimental and observed changes in climate. *Ecology*, **76**, 694–711.

Clarke KR, Gorley RN (2006) *Primer v6: User manual/tutorial*. PRIMER-E Ltd, Plymouth, UK.

Clarke KR, Warwick RM (2001) *Change in Marine Communities: An Approach to Statistical Analysis and Interpretation*, 2nd edn. PRIMER-E, Plymouth, UK.

Coplen TB (1996) New guidelines for reporting stable hydrogen, carbon, and oxygen isotope-ratio data. *Geochimica et Cosmochimica Acta*, **60**, 3359–3360.

Craig H (1961) Isotopic variations in meteoric waters. *Science*, **133**, 1702–1703.

Craig H, Gordon LI (1965) Deuterium and oxygen 18 variations in the ocean and the marine atmosphere. *Stable Isotope in Oceanographic Studies and Paleotemperatures*, (ed. Tongiorgi E), pp. 9–130. Pisa, Italy, Laboratorio di Geologia Nucleare, Pisa, Italy.

Eastman JR (2009) *IDRISI Taiga, Guide to GIS and Remote Processing*, Clark University, Worcester, MA, USA.

Environment Canada (2009) National Climate Data and Information Archive. Available at : http://www.climate.weatheroffice.ec.ge.ca/climateData/hourlydata_e.html (accessed 1 November 2009).

Epstein S, Mayeda T (1953) Variation of O^{18} content of waters from natural sources. *Geochimica et Cosmochimica Acta*, **4**, 213–224.

Gat JR, Bowser C (1991) The heavy isotope enrichment of water in coupled evaporative systems. In: *Stable Isotope Geochemistry: A Tribute to Samuel Epstein* (eds Taylor HP, O'Neil JR, Kaplan IR), pp. 159–168. Special Publication, The Geochemical Society, San Antonio.

Geldsetzer T, Sanden JVD, Brisco B (2010) Monitoring lake ice during spring melt using RADARSAT-2 SAR. *Canadian Journal of Remote Sensing*, **36**, S391–400.

Gibson JJ (2002) A new conceptual model for predicting isotopic enrichment in lakes in seasonal climates. *PAGES News*, **10**, 10–11.

Gonfiantini R (1986) Environmental isotopes in lake studies. In: *Handbook of Environmental Isotope Geochemistry*, Vol. **2** (eds Fritz P, Fontes JC), pp. 113–168. Elsevier, New York, USA.

Hinkel KM, Jones BM, Eisner WR, Cuomo CJ, Beck RA, Frohn R (2007) Methods to assess natural and anthropogenic thaw lake drainage on the western Arctic coastal plain of northern Alaska. *Journal of Geophysical Research*, **112**, F02S16.

Hobbie SE, Chapin FS (1998) The response of tundra plant biomass, above-ground production, nitrogen, and CO_2 flux to experimental warming. *Ecology*, **79**, 1526–1544.

Hudson J, Henry G, Cornwell K (2011) Taller and larger: shifts in Arctic tundra leaf traits after 16 years of experimental warming. *Global Change Biology*, **17**, 1013–1021.

Jepsen SM, Voss CI, Walvoord MA, Rose JR, Minsley BJ, Smith BD (2013) Sensitivity analysis of lake mass balance in discontinuous permafrost: the example of disappearing Twelvemile Lake, Yukon Flats, Alaska (USA). *Hydrogeology Journal*, **21**, 185–200.

Jones BM, Arp CD, Hinkel KM, Beck RA, Schmutz JA, Winston B (2009) Arctic lake physical processes and regimes with implications for winter water availability and management in the National Petroleum Reserve Alaska. *Environmental Management*, **43**, 1071–1084.

Jones BM, Grosse G, Arp CD, Jones MC, Walter Anthony KM, Romanovsky VE (2011) Modern thermokarst lake dynamics in the continuous permafrost zone, northern Seward Peninsula, Alaska. *Journal of Geophysical Research*, **116**, G00M03.

Jorgenson MT, Shur YL, Pullman ER (2006) Abrupt increase in permafrost degradation in Arctic Alaska. *Geophysical Research Letters*, **33**, L02503.

Kattsov VM, Källén E, Cattle HP *et al*. (2005) Future climate change: modeling and scenarios for the Arctic. In: *Arctic Climate Impact Assessment*, (eds. Symon C, Arris L, Heal B) pp. 99–150. Cambridge University Press, Cambridge, UK.

Krasting JP, Broccoli AJ, Dixon K, Lanzante J (2013) Future changes in northern hemisphere snowfall. *Journal of Climate*, **26**, 7813–7828.

Labrecque S, Lacelle D, Duguay CR, Lauriol B, Hawkings J (2009) Contemporary (1951-2001) Evolution of Lakes in the Old Crow Basin, Northern Yukon, Canada: remote sensing, numerical modeling, and stable isotope analysis. *Arctic*, **62**, 225–238.

Lantz TC, Marsh P, Kokelj SV (2013) Recent shrub proliferation in the Mackenzie Delta uplands and microclimatic implications. *Ecosystems*, **16**, 47–59.

Liston G, Sturm M (1998) A snow-transport model for complex terrain. *Journal of Glaciology*, **44** (148), 498–516.

MacDonald LA, Turner KW, Balasubramaniam AM, Wolfe BB, Hall RI, Sweetman JN (2012) Tracking hydrological responses of a thermokarst lake in the Old Crow Flats (Yukon Territory, Canada) to recent climate variability using aerial photographs and paleolimnological methods. *Hydrological Processes*, **26**, 117–129.

Mackay JR (1988) Catastrophic lake drainage, Tuktoyaktuk Peninsula area, District of Mackenzie. In: *Current Research, Part D*, Geological Survey of Canada, Paper 88-1D, pp. 83–90.

Mackay JR (1999) Periglacial features developed on the exposed lake bottoms of seven lakes that drained rapidly after 1950, Tuktoyaktuk Peninsula area, western Arctic coast, Canada. *Permafrost and Periglacial Processes*, **10**, 39–63.

Marsh P, Neumann NN (2001) Processes controlling the rapid drainage of two ice-rich permafrost-dammed lakes in NW Canada. *Hydrological Processes*, **15**, 3433–3446.

Marsh P, Bartlett P, MacKay M, Pohl S, Lantz T (2010) Snowmelt energetics at a shrub tundra site in the western Canadian Arctic. *Hydrological Processes*, **24**, 3603–3620.

McFadden JP, Liston GE, Sturm M, Pielke RA, Chapin FS (2001) Interactions of shrubs and snow in arctic tundra: measurements and models. In: *Soil-Vegetation-Atmosphere Transfer Schemes and Large-Scale Hydrological Models* (eds Dolman AJ, Hall AJ, Kavvas ML, Oki T, Pomeroy JW), pp. 317–325. International Association of Hydrological Sciences, Wallingford, UK.

Morrison J, Brockwell T, Merren T, Fourel F, Phillips AM (2001) On-line high-precision stable hydrogen isotopic analyses on nanoliter water samples. *Analytical Chemistry*, **73**, 3570–3575.

Myers-Smith IH, Forbes BC, Wilmking M *et al.* (2011) Shrub expansion in tundra ecosystems: dynamics, impacts and research priorities. *Environmental Research Letters*, **6**, 045509.

Osterkamp T, Romanovsky VE (1999) Evidence for warming and thawing of discontinuous permafrost in Alaska. *Permafrost and Periglacial Processes*, **10**, 17–37.

Payette S, Delwaide A, Caccianiga M, Beauchemin M (2004) Accelerated thawing of subarctic peatland permafrost over the last 50 years. *Geophysical Research Letters*, **31**, L18208.

Plug L, Walls C, Scott B (2008) Tundra lake changes from 1978 to 2001 on the Tuktoyaktuk Peninsula, western Canadian Arctic. *Geophysical Research Letters*, **35**, L03502.

Pohl S, Marsh P, Onclin C, Russell M (2009) The summer hydrology of a small upland tundra thaw lake: implications to lake drainage. *Hydrological Processes*, **23**, 2536–2546.

Pomeroy J, Marsh P, Gray D (1997) Application of a distributed blowing snow model to the Arctic. *Hydrological Processes*, **11**, 1451–1464.

Porter TJ, Pisaric MFJ (2011) Temperature-growth divergence in white spruce forests of Old Crow Flats, Yukon Territory, and adjacent regions of northwestern North America. *Global Change Biology*, **17**, 3418–3430.

Prowse T, Wrona F, Reist J, Gibson J, Hobbie J, Lévesque L, Vincent W (2006) Climate change effects on hydroecology of Arctic freshwater ecosystems. *AMBIO: A Journal of the Human Environment*, **35**, 347–358.

R Core Team (2013) *R: A Language and Environment for Statistical Computing*. R Foundation for Statistical Computing, Vienna, Austria. Available at: http://www.R-project.org/ (accessed 4 September 2013).

Riordan B, Verbyla D, McGuire AD (2006) Shrinking ponds in subarctic Alaska based on 1950–2002 remotely sensed images. *Journal of Geophysical Research G: Biogeosciences*, **111**, G04002.

Roach J, Griffith B, Verbyla D, Jones J (2011) Mechanisms influencing changes in lake area in Alaskan boreal forest. *Global Change Biology*, **17**, 2567–2583.

Rover J, Ji L, Wylie BK, Tieszen LL (2012) Establishing water body areal extent trends in interior Alaska from multi-temporal Landsat data. *Remote Sensing Letters*, **3** (7), 595–604.

Rowland JC, Jones CE, Altmann G *et al.* (2010) Arctic landscapes in transition: responses to thawing permafrost. *EOS, Transactions American Geophysical Union*, **91**, 26–29.

Roy-Léveillée P, Burn CR (2010) *Permafrost conditions near shorelines of oriented lakes in Old Crow Flats, Yukon Territory*. Proceedings Canadian Geotechnical Conference - Calgary, Alberta, pp. 1509–1516.

Schindler D, Smol JP (2006) Cumulative effects of climate warming and other human activities on freshwaters of arctic and subarctic North America. *AMBIO: A Journal of the Human Environment*, **35**, 160–168.

Smith L, Sheng Y, MacDonald G, Hinzman L (2005) Disappearing arctic lakes. *Science*, **308**, 1429.

Smol JP, Douglas MSV (2007) Crossing the final ecological threshold in high Arctic ponds. *Proceedings of the National Academy of Sciences of the United States of America*, **104**, 12395–12397.

Sturm M, McFadden JP, Liston GE, Chapin FS, Racine CH, Holmgren J (2001) Snow-shrub interactions in Arctic tundra: a hypothesis with climatic implications. *Journal of Climate*, **14**, 336–344.

The Ramsar Convention on Wetlands (1982) List Available at: http://www.ramsar.org/cda/en/ramsar-documents-list/main/ramsar/1-31-218_4000_0 (accessed 30 October 2009).

Thornthwaite C (1948) An approach toward a rational classification of climate. *The Geographical Review*, **38**, 1–94.

Turner KW, Wolfe BB, Edwards TWD (2010) Characterizing the role of hydrological processes on lake water balances in the Old Crow Flats, Yukon Territory, Canada, using water isotope tracers. *Journal of Hydrology*, **386**, 103–117.

Wolfe BB, Light EM, Macrae ML *et al.* (2011a) Divergent hydrological responses to 20th century climate change in shallow tundra ponds, western Hudson Bay Lowlands. *Geophysical Research Letters*, **38**, L23402.

Wolfe BB, Humphries M, Pisaric M *et al.* (2011b) Environmental change and traditional use of the Old Crow Flats in northern Canada: an IPY opportunity to meet the challenges of the new northern research paradigm. *Arctic*, **64**, 127–135.

Yi Y, Brock BE, Falcone MD, Wolfe BB, Edwards TWD (2008) A coupled isotope tracer method to characterize input water to lakes. *Journal of Hydrology*, **350**, 1–13.

Yoshikawa K, Hinzman L (2003) Shrinking thermokarst ponds and groundwater dynamics in discontinuous permafrost near Council, Alaska. *Permafrost and Periglacial Processes*, **14**, 151–160.

Supporting Information

Additional Supporting Information may be found in the online version of this article:

Table S1. Measured and modeled values used to calculate the Local Evaporation Line for Old Crow Flats, YT. E/I and δ_I calculations are based on parameters determined for individual years.

Table S2. General statistics (i.e., minimum, maximum, range, and mean) of isotope data for each sampling campaign.